

Three-dimensional common-path interferometer for AIC: nulling of polychromatic light

A. V. Tavrov¹, Yu. Otani¹,
T. Kurokawa¹ and M. Takeda²

¹Tokyo University of Agriculture and Technology,
2-24-16, Nakamachi, Koganei-shi, Tokyo, Japan
email: tavrov@cc.tuat.ac.jp

²The University of Electro-Communications,
1-5-1, Chofugaoka, Chofu, Tokyo, Japan
email: takeda@ice.ucc.ac.jp

Abstract. Three-dimensional common-path interferometer is proposed to obtain achromatic nulling for the on-axial source; the off-axial source remains detectable. The 3D interferometer involves $\pm 90^\circ$ polarization rotations in each interferometer arm. That results in the achromatic 180° phase shift, so that the on-axial source interferes destructively. Depending on the source axial position, the light energy is split by different ratios between the Bright and the Nulled interferometer outputs. For the linearly polarized on-axial source, all the energy at nearly 100% is directed to the Bright port. For the off-axial source, the light is split by the ratio at nearly 50%/50% between the Bright and the Nulled ports. The common-path scheme compensates effectively the optical path difference (OPD) and it remains stable to mechanical vibrations. Theory, simulations and preliminary breadboard experiments are shown to be in reasonable agreement.

Keywords. Nulling interferometry, coronagraphy, common-path interferometry, achromatic nulling, mechanical stability.

1. Introduction

Achromatic photonic devices are in demand in variety of optical metrology applications from ultra-short pulse laser beams, to radar techniques and astronomical instrumentation Serabyn, Wallace, *et al.* (1999); Baudoz, Rabbia & Gay (2000); Baba, Murakami & Ishigaki (2001). A star emits in 10^7 – 10^{10} more light energy than the illuminating target planet depending on the wavelength band. Referring to the concept by Bracewell (1978), the long-base interferometry presents a high angular resolution technique in which the light from on-axial bright source is destructively interfering, when an off-axial low intensity target interferes constructively or remains not eliminated and therefore can be detected. To realize this principle, many schemes have been recently proposed, among which are phase masks, Rouan, *et al.* (2000), and pupil masks, delay lines arrays, Avoort, Mieremet, Pereira & Braat (2004), achromatic phase shifters, Rabbia, Gay, Bascou & Schneider (2001), and their sophisticated combinations Nishikawa, Kotani, Murakami, Baba, Itoh & Tamura (2005), just to mention a few. Among others, a fully achromatic π -shifter is a key device indispensable for the instrumentation of nulling interferometry and coronagraphy.

In the achromatic interfero-coronagraph, Baudoz, Rabbia & Gay (2000), in the Michelson interferometer, the both arms have to be adjusted accurately at the zero OPD, which

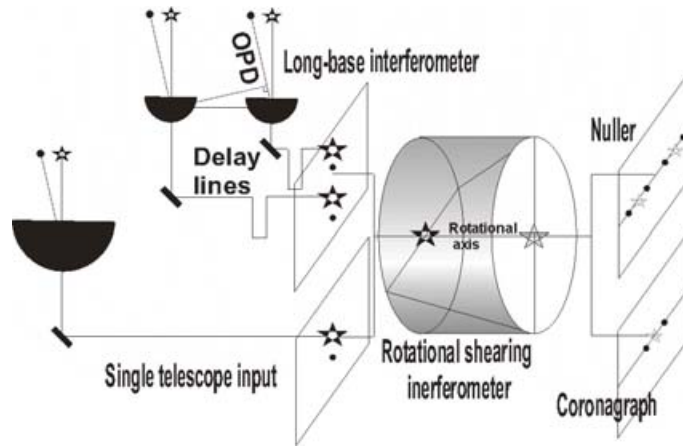


Figure 1. Nulling principle for long-base interferometry and coronagraphy.

is hard to realize with a mechanically unstable non-common-path interferometer. In this paper, a recently proposed common-path interferometer scheme, Tavrov, Tanaka, Shioda, Kurokawa & Takeda (2004), is analyzed, which effectively maintains the OPD between the interferometer arms and simultaneously adds an achromatic π -phase shift for destructive interference. For linearly polarized light, aside from the reflection losses on the mirrors, the interferometer throughput is enhanced then in the previous scheme, Tavrov, Bohr, Totzeck, Tiziani & Takeda (2002); for an on-axial source it can attain nearly a 100-to-0 percent power split ratio at the two exit ports of the interferometer, which are referred to Bright and Nulled ports, respectively. For an off-axial source, equal power comes out from the two ports with nearly 50-to-50 percent split ratio.

2. Combination of two beams with 180° RSI scheme

Let us explain, how, by means of the nulling interferometry, the light from an on-axial strong source is reduced via destructive interference, and how, by contrast, an off-axial faint source remains detectable. As shown in Figure 1, the OPD between two interferometer arms is equal to zero for on-axial source, denoted by star-mark. Its destructive interference occurs after the achromatic π - phase shifter by means of 180° RSI (rotational shearing interferometer), Serabyn, Wallace, *et al.* (1999); Scholl & Paez (1999). RSI means a differential interferometer with some rotation of the copied wavefront. A similar wavefront folding system was extensively studied by Itoh (1996) with a very small amount of the rotational shear. In Figure 1, shown by o-mark, the off-axial source introduces a non-zero optical path difference, its interference becomes no longer destructive and such an off-axial source can be detected. Both the stellar coronagraph and the long-base interferometer can use the proposed interferometer as an achromatic nulling beamcombiner.

3. Optical scheme

Conventional Sagnac interferometer, Hariharan (1995), maintains the OPD because of two interferometer arms are designed within the common path. For the nulling purpose, the Sagnac interferometer is extended in 3D, its optical scheme is shown in Figure 2.

This interferometer introduces $\pm 90^\circ$ polarization rotations along the *forward* and the *backward* light paths. Three-dimensional mirror train consists of six plane mirrors

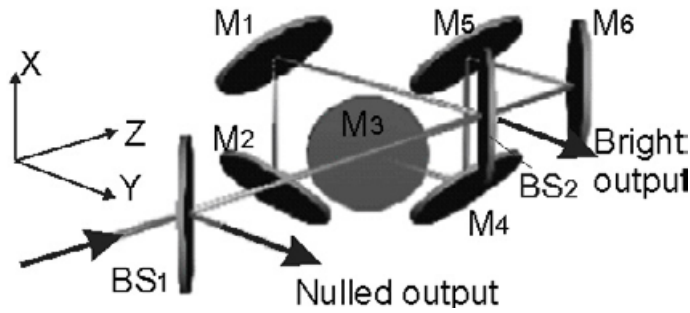


Figure 2. Out-of-plane common-path interferometer.

denoted consequently by $M_{1..6}$ and two beamsplitters: BS_1 , BS_2 . Principal rays are shown along the optical axis. Let us define the forward propagation following the route $BS_1 - BS_2 - M_1 - M_2 - M_3 - M_4 - M_5 - M_6 - BS_2 - BS_1$ that is the first interferometer arm. The backward path: $BS_1 - BS_2 - M_6 - M_5 - M_4 - M_3 - M_2 - M_1 - BS_2 - BS_1$ introduces the second interferometer arm. Local p- and s- planes of the mirrors $M_{1..6}$ and the beamsplitter BS_2 are oriented *out-of-plane*, Tavrov, Miyamoto, Kawabata, Takeda & Andreev (2000) and cause $\pm 90^\circ$ polarization rotations in the first and the second interferometer arms correspondingly. In respect each other, the images in the arms become geometrically rotated to 180° . Electrical vectors follow the image rotation and it introduces the π -phase shift for destructive interference.

This is similar to the effect in the existing AIC scheme, Baudoz, Rabbia & Gay (2000), where one interferometer arm contains the plane mirror train and another arm contains the propagation through the focus so two images are superimposed, and flipped to 180° each to other.

To achieve a dark field, both interfering beams must have equal intensities, which is not realized in the common case by splitting and combining of the beams. An actual beam splitter works chromatically because it introduces different amounts of transmission \mathbf{T} and reflection \mathbf{R} , and the ratio depends on the wavelength. Following the reference, Serabyn, Wallace, *et al.* (1999), this problem is solved, making possible splitting and combining of beams with the equal \mathbf{RT} and \mathbf{TR} products.

Interference process always satisfies the energy conservation law, therefore in our scheme one BS_2 port reflects the light energy resulted by constructive interference and is denoted as the “**Bright output**”. Another BS_2 port transmits the rest light energy resulted by destructive interference to the “**Nulled output**”. The nulled output faced back to the incident light direction and the nulled result is observed via BS_1 . To enhance the RSI transmittance for coronagraphy, the BS_1 is designed as the broadband polarization beamsplitter (PBS). Its transmitting mode is set matching with the incident linear polarization state on the input therefore nearly complete energy flux can be entered into the interferometer. Interferometer arms rotate the input polarization to $\pm 90^\circ$ so the light polarization which is returned back to the BS1 matches now with the reflection mode of the PBS and again nearly complete energy flux can be directed to the Nulled output. Following the geometrical image rotation, the π -phase difference is added achronatically.

Ray tracing shows that an off-axial light component has another interference result: each tilted wave results in two images, which are spatially separated, as shown in Figure 1. They do not interfere because they are geometrically separated. By the closer axial position than the Airy diameter (close-sensing), Baudoz, Rabbia & Gay (2000), some

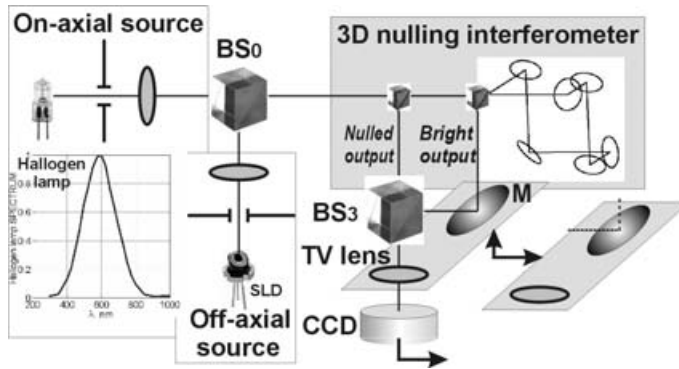


Figure 3. Experimental scheme.

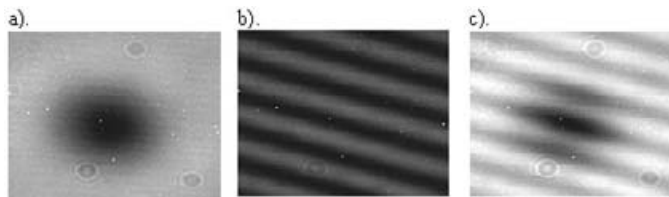


Figure 4. Pupil domain interference patterns: (a) *extended* on-axis source, (b) off-axis source, (c) superposition of the on-axis source and the off-axis source.

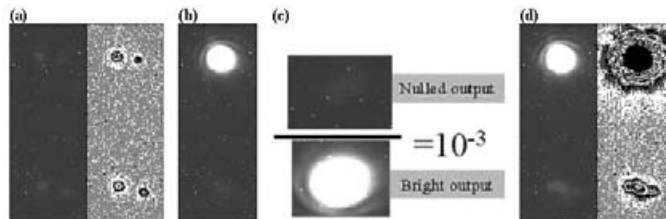


Figure 5. Achromatic nulling, the *Bright output* is above the *Nulled output*. (a) – Off-axis source is switched on. (b) – On-axis source is switched on. (c) – Intensity values were summed up in zooms, the nulling depth is about 10^{-3} . (d) – Both the on-axis and the off-axis sources are switched on.

of their fractions still interfere destructively, hence some non-interfering fractions cause the target light amount that is not nulled and can be detected. Due to the propagations forward and back, the proposed design compensates chromaticities of the beamsplitter and the mirrors. Achromatic phase shift between two interferometer arms is shown equal to 180° and the interference contrast of 100% is possible.

4. Experiment

In order to confirm an achromatic nulling property introduced by the proposed 3D common-path interferometer by simple experiments, we have constructed the bread-boarded demonstrator, its optical set-up is shown in the Figure 3. We made use of two separate light sources: the halogen lamp and the super-luminescent diode (SLD). The halogen lamp has emitted the spectral width over 300 nm, it was used to construct the on-axis source. The SLD emitting the light over 20 nm spectral width was used to construct the off-axis source. In order to obtain spatially coherent illumination we

have constructed the spatial filters. Light from halogen lamp was transferred through the pinhole with the nearly $5\ \mu\text{m}$ effective diameter, which was placed in the 6 mm focus of achromat lens. Second source shows the effective angular size about 4 arc minutes. SLD light was coupled into single-mode fiber and emitted by commercial fiber collimator. SLD source shows smaller angular size. The sources were aligned on-axially and off-axially and were combined by use of the beamsplitter BS_0 ; their lights can be clearly identified in the pupil space, Figure 4: (a) – central dark *ring-shaped* fringe was caused by the on-axial (extended) source; (b) – the fringes with more dense spacing are originated from the off-axial source tilted about 10 arcminutes; (c) – both the on-axial and the off-axial sources are superimposed, their fringes localizations have both the destructive interference on-axis. However the more dense fringes are caused by the off-axial source and we can detect its light on the background of the strong on-axial source, which is mostly suppressed due to destructive interference. Some residual energy remains non-nulled due to the finite size of the on-axial source and due to misalignments.

In order the CCD observes the image space, we converted the interference patterns from the pupil space to the image space attaching the TV lens, which focuses the light on the CCD. For demonstration purposes, we combined by the BS_3 two interferometer output ports: the Nulled and the Bright within the same CCD frame, Figure 3. We aligned the Nulled and Bright images one above the other: the upper image area corresponds to the Bright output and in the bottom is the Nulled output.

In Figure 5 (a) – the only off-axial source is switched on and we observe its image in both areas: in the Nulled output and in the Bright output. Off-axial source is presented as the two pair of images, each with 0.25 fraction, located symmetrically from the RSI optical axis. We set low intensity for the off-axial light; shown on right, it is contrasted by another palette on the CCD thermal noise background. In (b), the only on-axial source is switched on, emitting relatively strong light intensity; anyway this intensity and the CCD exposure time have been optimized in order to omit the CCD saturation. We see the strong signal in the upper Bright area (shown saturated). In the bottom Nulled area we can still detect some amount of residual energy. In order to estimate the Nulling efficiency, in (c) we compare the Nulled and the Bright areas. Their pixel intensities have been summed up and their ratio is equal to coronagraphy contrast $\approx 10^{-3}$ was measured, which makes the reasonable nulling efficiency for the used sources size of several arcminutes. In (d), the both on-axial and off-axial sources are shown superimposed, here in the upper Bright area, the intensive on-axial component saturates the CCD and in Nulled area, the weak off-axial source can be visually separated. The CCD exposure time in Figure 5 (a), (b), (c) was set at 2 minutes, in Fig. 5 (d) was set at 4 minutes, that can demonstrate the mechanical stability of the system.

5. Conclusions

We proposed the three-dimensional (out-of-plane) common-path interferometer for the achromatic nulling. Both the computer simulations and the experiments show the reasonable agreement to demonstrate the achromatic nulling of the on-axial light. The nulling efficiency is affected if the interferometer mirrors are misaligned; anyway it is possible to obtain the 10^{-10} achromatic nulling for the on-axial source. We have constructed breadboard demonstrator and have obtained the nulled images with the white-light of the spectral width over 300 nm in visible range. For the used in our experiment, the *giant* source size of several arcminutes, we show experimentally the achromatic nulling depth around of 10^{-3} .

Acknowledgements

This work is a part of the 21st Century COE program on “Future Nano-Materials” conducted in the Tokyo University of Agriculture and Technology. We thank Y. Rabbia from the Observatoire de la Cote d’Azur and Ju. Nishikawa and M. Tamura from the National Astronomical Observatory Japan for helpful suggestions and discussions.

References

- Serabyn, E., Wallace, J. K., Hardy, G. J., Schmidlin, E. G. H., & Nguyen, H. T. 1999, “Deep nulling of visible laser light,” *Appl. Optics* 38, 712
- Baudoz, P., Rabbia, Y., & Gay, J. 2000, “Achromatic interfero coronagraphy,” *Astron. Astrophys. Suppl. Ser.* 141, 319–329
- Baba, N., Murakami, N., & Ishigaki, T. 2001, “Nulling interferometry by use of geometric phase,” *Opt. Lett.* 26, 1167
- Bracewell, R. N. 1978, *Nature* 274, 780
- Rouan, D., Riaud, P., Boccaletti, A., Clenet, Y., & Labeyrie, A. 2000, “The four-quadrant phase mask coronagraph,” *Publications of the Astronomical Society of the Pacific*. 112, 1479–1486
- C. van der Avoort, Mieremet, A., Pereira, S., & Braat, J. 2004, “Demonstration of nulling using delay line phase shifters,” *In New Frontiers in Stellar Interferometry, ed. by W. Traub, Proc. SPIE* 5491, 816
- Rabbia, Y., Gay, J., Bascou, E., & Schneider, J. L. 2001, *contract14398/00/NL/MV report European Space Research and Technology Centre, Noordwijk, Holland, rabbia@obs-azur.fr*
- Nishikawa, Ju., Kotani, T., Murakami, N., Baba, N., Itoh, Y., & Tamura, M. 2005, “Combination of nulling interferometer and modified pupil for observations of exo-planets,” *A&A* 379–384
- Tavrov, A., Tanaka, Yo., Shioda, T., Kurokawa, T., & Takeda, M. 2004, “Achromatic coronagraph based on out-of-plane common-path nulling interferometer,” *in New Frontiers in Stellar Interferometry, ed. Wesley A. Traub, Proc. SPIE* 5491, 824
- Tavrov, A., Bohr, R., Totzeck, M., Tiziani, H., & Takeda, M. 2004, “Achromatic nulling interferometer based on a geometric spin-redirected phase,” *Optics Letters* 27, 2070
- Scholl, M. S. & Paez, G. 1999, “Cancellation of star light generated by a nearby star-planet system upon detection with a rotationally-shearing interferometer,” *Infrared Physics and Technology* 40, 357
- Itoh, K. 1996, “Interferometric Multispectral Imaging,” *In E. Wolf, Progress in Optics XXXV*, 145
- Hariharan, P. 1995, “Interferometers,” *Handbook of Optics 2, M. Bass, McGraw-Hill, New York*
- Tavrov, A., Miyamoto, Yo., Kawabata, T., Takeda, M., & Andreev, V. 2000, “Generalized algorithm for the unified analysis and simultaneous evaluation of geometrical spin-redirected phase and Pancharatnam phase in a complex interferometric system,” *JOSA A* 17, 1, 154